

RESEARCH PAPER

## Co<sub>3</sub>O<sub>4</sub> Nanoparticles : Synthesis, Characterization and Its Application as Performing Anode in Li-Ion Batteries

Aliakbar Dehno Khalaji <sup>1\*</sup>, Marketa Jarosova <sup>2</sup>, Pavel Machek <sup>2</sup>, Kunfeng Chen <sup>3</sup>, Dongfeng Xue <sup>3</sup>

<sup>1</sup> Department of Chemistry, Faculty of Science, Golestan University, Gorgan, Iran

<sup>2</sup> Institute of Physic of the Czech Academy of Sciences, v.v.i., Na Slovance 2, 182 21 Prague 8, Czech Republic

<sup>3</sup> State Key Laboratory of Rare Earth Resource Utilization, Changchun Institute of Applied Chemistry, Chinese Academy of Sciences, Changchun 130022, China

### ARTICLE INFO

#### Article History:

Received 11 March 2020

Accepted 05 June 2020

Published 01 July 2020

#### Keywords:

Calcination

Electrochemical performance

Li-Ion batteries

Nanoparticles

### ABSTRACT

In this research, a convenient, simple and rapid route for the preparation of Co<sub>3</sub>O<sub>4</sub> nanoparticles using the calcination of Co(NO<sub>3</sub>)<sub>2</sub>·6H<sub>2</sub>O at the presence of benzoic acid (1:1 weight ratio) is reported. Further, the as-prepared Co<sub>3</sub>O<sub>4</sub> nanoparticles were characterized by X-ray powder diffraction (XRD) and transmission electron microscopy (TEM). XRD result confirmed the Co<sub>3</sub>O<sub>4</sub> nanoparticles are pure phase and the average crystallite size for Co<sub>3</sub>O<sub>4</sub> nanoparticles was found 77 nm. The TEM images reveal nanoparticles with size ranging from 50 to 100 nm, which is in conformity with the calculation of average crystallite sizes from XRD patterns. Furthermore, the prepared Co<sub>3</sub>O<sub>4</sub> nanoparticles were investigated as an anode material for Li-ion batteries. Results showed that the Co<sub>3</sub>O<sub>4</sub> nanoparticles exhibited excellent electrochemical performance and cycling stability, a capacity of 1127 mA h g<sup>-1</sup> was obtained at 100 mA g<sup>-1</sup> and the samples exhibited stable discharge behavior up to 130 cycles with high rate capability.

### How to cite this article

Dehno Khalaji AA., Jarosova M., Machek P., Chen K., Xue D. Co<sub>3</sub>O<sub>4</sub> Nanoparticles : Synthesis, Characterization and Its Application as Performing Anode in Li-Ion Batteries. J Nanostruct, 2020; 10(3): 607-612. DOI: 10.22052/JNS.2020.03.014

### INTRODUCTION

Recently, study of transition metal oxide (TMO) nanoparticles and nanocomposites as cathode [1-3] or anode [4-13] materials for rechargeable Li-ion batteries (LIB) has been one of the best hot research topics, because the preparation of TMO nanoparticles is often simple, low-cost and rapid. The transition metal oxide (TMO) nanoparticles as anode materials have also excellent electrochemical performance and cycling stability [1-13]. Nanoparticles of Co<sub>3</sub>O<sub>4</sub> can be prepared by various techniques, i.e. solid-state thermal decomposition [14] or carbon assisted decomposition [15,16], and show variety of properties that are favorable in applications such

as degradation of organic dye [14], oxidation of alcohols [15], selective oxidation of alcohols [16] and electrocatalytic oxidation of H<sub>2</sub>O<sub>2</sub> [17]. Among various transition metal oxides studied for Li ion batteries, LIB's with cobalt oxide nanoparticles as anode have higher energy density compared with the other energy storage devices [5-13]. Unfortunately, nanoparticles of Co<sub>3</sub>O<sub>4</sub> show large volume changes during repeated lithiation and delithiation processes [9]. However, they have higher capacity (about 890 mA h g<sup>-1</sup>) [5-13] than graphite (370 mA h g<sup>-1</sup>). In recent years, various shapes of Co<sub>3</sub>O<sub>4</sub> nanostructures such as nanoring, mesoporous, 3D nanofiber and nanofilms have been prepared and studied as anode materials

\* Corresponding Author Email: [alidkhalaji@yahoo.com](mailto:alidkhalaji@yahoo.com)

extensively [5-13]. For example mesoporous Co<sub>3</sub>O<sub>4</sub> network that has been prepared by Wen *et al.* *via* thermal decomposition of an amorphous metal complex exhibits excellent performance for Li storage [8]. Su *et al.* prepared Co<sub>3</sub>O<sub>4</sub> hexagonal nanorings *via* treating Co-based metal organic frameworks [9]. Co<sub>3</sub>O<sub>4</sub> hexagonal nanorings show the specific capacity of 1370 mA h g<sup>-1</sup> after 30 cycles. Gurunathan *et al.* reported convenient synthesis route for preparation of Co<sub>3</sub>O<sub>4</sub> hollow microsphere [10] that exhibited excellent electrochemical performance (915 mA h g<sup>-1</sup>) and cycling stability (350 cycles).

This study is a part of our ongoing effort to prepare transition metal oxide nanoparticles and investigated them as Li-ion batteries [18,19]. Herein, we report a convenient, simple and rapid method for preparation of Co<sub>3</sub>O<sub>4</sub> nanoparticles using the calcination of Co(NO<sub>3</sub>)<sub>2</sub>·6H<sub>2</sub>O at the presence of benzoic acid. Served as Li-ion battery anode, Co<sub>3</sub>O<sub>4</sub> nanomaterials show high electrochemical performance.

## MATERIALS AND METHODS

All compounds used in this research were purchased from Merck Company and used without any purification. The XRD patterns were obtained on Empyrean powder diffractometer of PANalytical in Bragg-Brentano configuration equipped with a flat sample holder and PIXcel3D detector (Cu K $\alpha$  radiation,  $\lambda = 1.5418 \text{ \AA}$ ). TEM images were recorded with the transmission electron microscope Philips CM120 with a LaB6 cathode operating at 120 kV and equipped with CCD camera Olympus Veleta

### Synthesis of Co<sub>3</sub>O<sub>4</sub> nanoparticles

1 g of Co(NO<sub>3</sub>)<sub>2</sub>·6H<sub>2</sub>O and 1 g of benzoic acid were put into a crucible and ground together for 5 min. The mixture was then annealed at 600 °C in air for 3 h. The black products were rinsed with water and finally dried at 65 °C for 12 h.

### Electrode preparation and electrochemical test method

The active Co<sub>3</sub>O<sub>4</sub> material was mixed with carbon black and PVDF at a mass ratio of 70:15:15 to form slurry with NMP as solvent. The slurry was then spread onto Cu foil by doctor-blade, and dried at 80 °C for 12 h. The disc with diameter 1.53 cm was cut from dried Cu foil, and compressed under the

pressure of 10 MPa to form a working electrode. The loading of active material on Cu foil was about 1 mg cm<sup>-2</sup>. Lithium metal was used as the counter and the reference electrode. The electrodes were assembled into a coin cell (CR2032) in an Ar-filled glovebox using Celgard 2400 as separator and 1 M LiPF<sub>6</sub> in ethylene carbonate/dimethyl carbonate/diethyl carbonate (EC/DMC/DEC, 1:1:1 vol%) as electrolyte. A galvanostatic cycling test of these assembled half-cells was conducted on a LAND CT2001A system in the voltage range of 0.01-3.0 V (vs. Li<sup>+</sup>/Li) at different current densities.

## RESULTS AND DISCUSSION

### XRD patterns

X-ray diffraction (XRD) pattern of Co<sub>3</sub>O<sub>4</sub> nanoparticles is shown on Fig. 1. In this pattern, there are several peaks at  $2\theta \approx 18.99^\circ$ ,  $31.26^\circ$ ,  $36.83^\circ$ ,  $38.54^\circ$ ,  $44.80^\circ$ ,  $55.64^\circ$ ,  $59.34^\circ$  and  $65.21^\circ$  which indicates the spinel with cubic face centered structure of Co<sub>3</sub>O<sub>4</sub> with standard diffraction data of card no. JCPDS = 01-080-1532. The structure was refined by Rietveld fit in crystallographic program Jana2006 [20] that confirmed the lattice parameter  $a = 8.085 \text{ \AA}$ . The size of crystallites was determined in the same program using fundamental parameter approach [21], which removed the instrumental part of the diffraction pattern by means of known geometry of the diffractometer. The average crystallite size for Co<sub>3</sub>O<sub>4</sub> nanoparticles was found 77 nm.

### TEM images

The morphology of Co<sub>3</sub>O<sub>4</sub> nanoparticles was characterized by TEM. The Fig. 2 shows the TEM images of the sample prepared at 600 °C. The images reveal nanoparticles with size ranging from 50 to 100 nm, which is in conformity with the calculation of average crystallite sizes from XRD patterns.

### Electrochemical properties

As shown in Fig. 3a, the reduction peak around 1.17, 0.92, 0.82 V in the first cycle can be associated with reduction of Co<sup>3+</sup>  $\rightarrow$  Co<sup>2+</sup>, Co<sup>2+</sup>  $\rightarrow$  Co and formation of Li<sub>2</sub>O and solid electrolyte interface (SEI) [5, 6]. The oxidation peak around  $\sim 2.0$  V can be attributed to the oxidation of Co  $\rightarrow$  Co<sub>3</sub>O<sub>4</sub> and decomposition of the SEI. In the following cycles, the redox peaks are well overlapped which means that Co<sub>3</sub>O<sub>4</sub> anode has high cycling performance

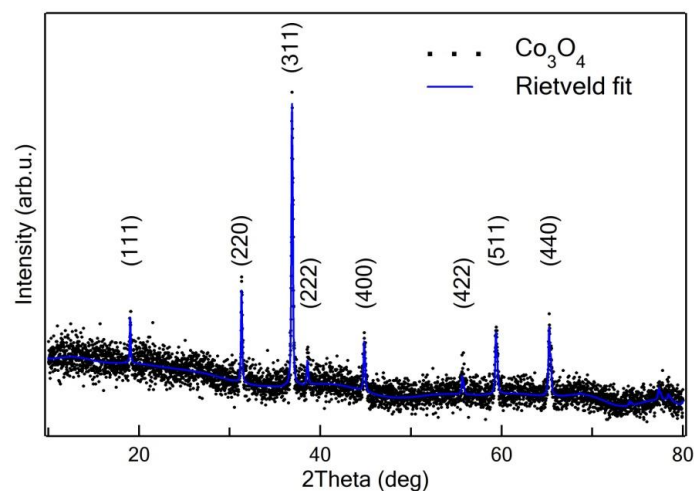


Fig. 1. XRD pattern of  $\text{Co}_3\text{O}_4$  nanoparticles.

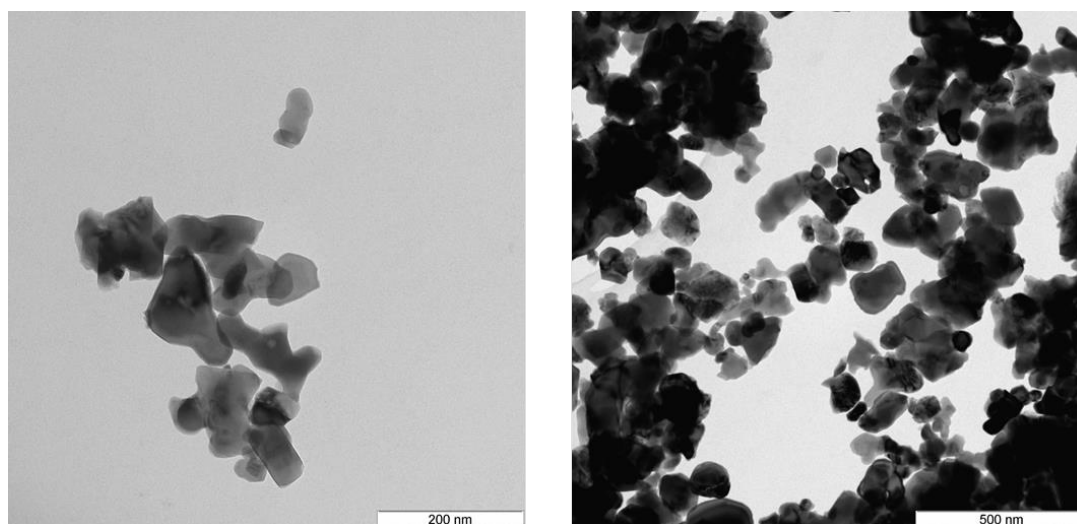


Fig. 2. TEM images of  $\text{Co}_3\text{O}_4$  nanoparticles at different magnifications

(Fig. 3b). Fig. 4 shows capacities at different current densities of  $100\text{--}1000\text{ mA g}^{-1}$ .  $\text{Co}_3\text{O}_4$  sample shows 1st discharge capacity of  $1996\text{ mA h g}^{-1}$  and charge capacity of  $1127\text{ mA h g}^{-1}$  [22]. The irreversible capacity loss is caused by the formation of SEI and electrolyte decomposition. At current density of  $1000\text{ mA g}^{-1}$ , the discharge capacity is  $380\text{ mA h g}^{-1}$ . The high capacity of the  $\text{Co}_3\text{O}_4$  electrodes can be attributed to high specific surface area which provides more active area that can react with  $\text{Li}^+$  ions [23,24]. The cycling performance was used to prove the stability of the as-formed samples. As shown in Fig. 4, the discharge capacity is  $868\text{ mA h}$

$\text{g}^{-1}$  after 130 charge-discharge cycles with capacity retention of 76%, compared with reversible capacity of  $1145\text{ mA h g}^{-1}$ . The decline of electrode performance may own to destroy of electrode materials or the change of electrode structure [25, 26].

The electrochemical impedance spectroscopy (EIS) was performed to show the resistance during electrochemical process [27]. Fig. 5 is the Nyquist plots of EIS with semicircle at high frequency and straight line at low frequency. The corresponding equivalent circuit is shown in inset of Fig. 5. The electrolyte resistance is  $2.3\text{ W}$ . The charge transfer

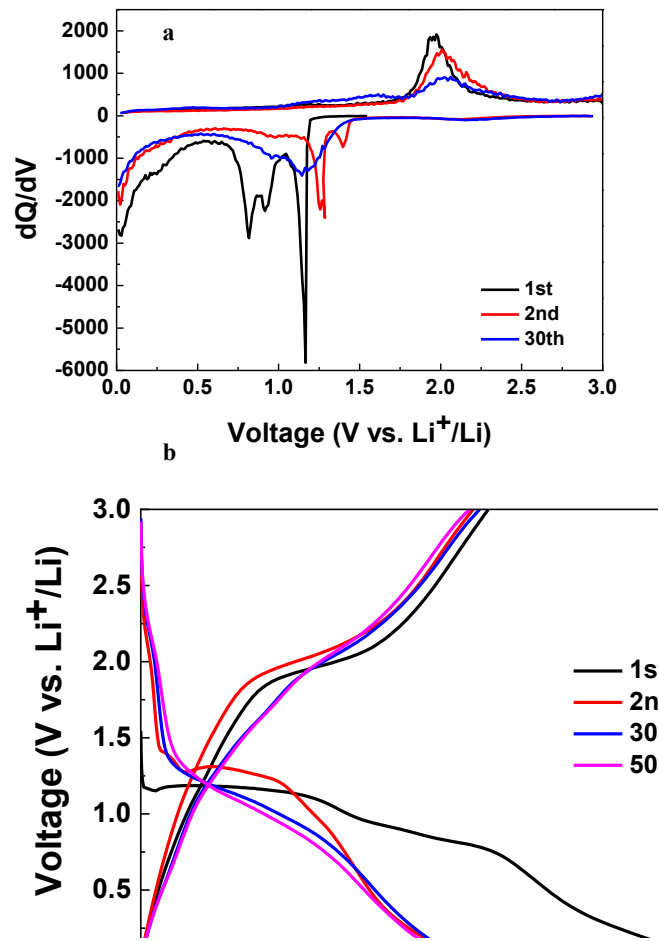


Fig. 3. Electrochemical Li-ion battery anode performance of  $\text{Co}_3\text{O}_4$  sample. (a) discharge-charge curves at current density of 100 mA/g. (b)  $dQ/dV$  curves with different cycling numbers.

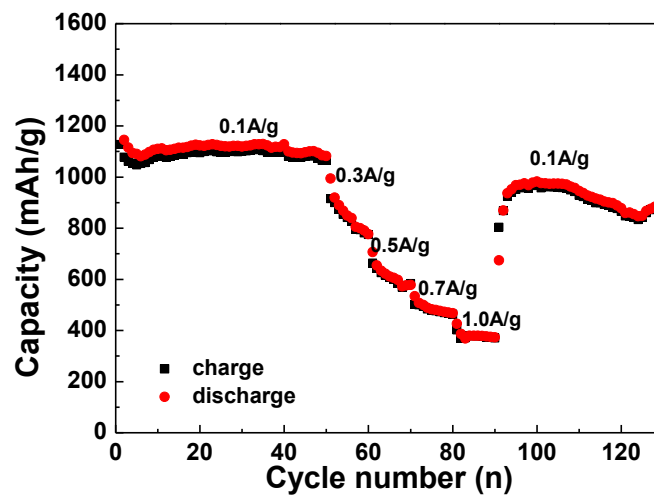


Fig. 4. Capacity of  $\text{Co}_3\text{O}_4$  at different current densities for Li-ion battery anode.

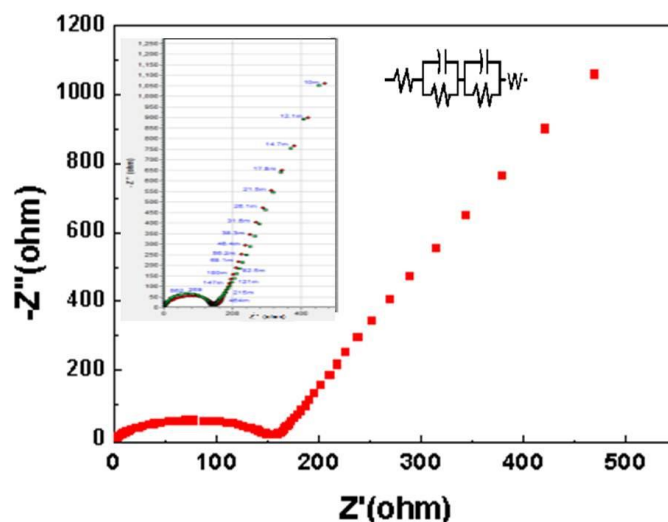


Fig. 5 Electrochemical impedance spectroscopy of Co<sub>3</sub>O<sub>4</sub> sample. Insets show equivalent circuit and fitting line.

Table 1. Li-ion batteries characteristics of Co<sub>3</sub>O<sub>4</sub> in literature and this work

| Materials   | capacity (mA h g <sup>-1</sup> ) | Charge-discharge cycles | Ref.      |
|---|----------------------------------|-------------------------|-----------|
| Co <sub>3</sub> O <sub>4</sub> nanoparticles        | 868                              | 130                     | This work |
| Co <sub>3</sub> O <sub>4</sub> particles            | 423                              | 40                      | 12        |
| Co <sub>3</sub> O <sub>4</sub> sheet                | 1245                             | 40                      | 28        |
| Co <sub>3</sub> O <sub>4</sub> rhombic dodecahedral | 1100                             | 6000                    | 29        |
| Co <sub>3</sub> O <sub>4</sub> nanocages            | 800                              | 30                      | 11        |
| Co <sub>3</sub> O <sub>4</sub> Chrysanthemum-loke   | 450                              | 50                      | 30        |
| Co <sub>3</sub> O <sub>4</sub> hexagonal nanoring   | 1370                             | 30                      | 9         |

resistances are 130 and 907 W in first and second circuits. Two RC circuits show that two interfaces may exist in this electrochemical system, for example SEI. The straight line represents Warburg diffusion process.

These electrochemical properties of the as-prepared Co<sub>3</sub>O<sub>4</sub> show that the good electrochemical performance with high storage capacity is comparable with the other previous works [9,11112,28-29]. In Table 1, previous reports about Co<sub>3</sub>O<sub>4</sub> based Li-ion batteries with different morphology are compared.

## CONCLUSION

In summary, Li-ion battery anodes based on Co<sub>3</sub>O<sub>4</sub> nanoparticles show better electrochemical performance. The 1st discharge capacity was 1996 mA h g<sup>-1</sup> and charge capacity was 1127 mA h g<sup>-1</sup>. Also, Co<sub>3</sub>O<sub>4</sub> sample shows decent cycle stability with specific capacities of about 868 mA h g<sup>-1</sup> at 100 mA g<sup>-1</sup> after 130 charge-discharge cycles. The high capacity of the Co<sub>3</sub>O<sub>4</sub> electrodes can be attributed

to high specific surface area which provides more active area that can react with Li<sup>+</sup> ions.

## ACKNOWLEDGMENTS

Financial support from the Golestan University and the National Natural Science Foundation of China (grant nos. 21521092), CAS-VPST Silk Road Science Found 2018 (GJHZ1854) is acknowledged. XRD and TEM analysis were supported by the project 18-10504S of the Czech Science Foundation using instruments of the ASTRA lab established within the Operation program Prague Competitiveness e project CZ.2.16/3.1.00/2451.

## CONFLICT OF INTEREST

The authors declare that there is no conflict of interests regarding the publication of this paper.

## REFERENCES

- Ghiyasiyan-Arani M, Salavati-Niasari M. Strategic design and electrochemical behaviors of Li-ion battery cathode nanocomposite materials based on AlV<sub>3</sub>O<sub>9</sub> with carbon

- nanostructures. *Composites Part B: Engineering*. 2020;183:107734.
- Gu M, Belharouak I, Zheng J, Wu H, Xiao J, Genc A, et al. Formation of the Spinel Phase in the Layered Composite Cathode Used in Li-Ion Batteries. *ACS Nano*. 2012;7(1):760-7.
  - Wang Z, Liu E, He C, Shi C, Li J, Zhao N. Effect of amorphous FePO<sub>4</sub> coating on structure and electrochemical performance of Li<sub>1.2</sub>Ni<sub>0.13</sub>Co<sub>0.13</sub>Mn<sub>0.54</sub>O<sub>2</sub> as cathode material for Li-ion batteries. *Journal of Power Sources*. 2013;236:25-32.
  - Wang X, Mao H, Shan Y. Enhanced photocatalytic behavior and excellent electrochemical performance of hierarchically structured NiO microspheres. *RSC Adv*. 2014;4(67):35614-9.
  - Shi Y, Pan X, Li B, Zhao M, Pang H. Co<sub>3</sub>O<sub>4</sub> and its composites for high-performance Li-ion batteries. *Chemical Engineering Journal*. 2018;343:427-46.
  - Fan L, Zhang W, Zhu S, Lu Y. Enhanced Lithium Storage Capability in Li-Ion Batteries Using Porous 3D Co<sub>3</sub>O<sub>4</sub> Nanofiber Anodes. *Ind Eng Chem Res*. 2017;56(8):2046-2053.
  - Wen W, Wu J-M, Cao M-H. Facile synthesis of a mesoporous Co<sub>3</sub>O<sub>4</sub> network for Li-storage via thermal decomposition of an amorphous metal complex. *Nanoscale*. 2014;6(21):12476-81.
  - Su P, Liao S, Rong F, Wang F, Chen J, Li C, et al. Enhanced lithium storage capacity of Co<sub>3</sub>O<sub>4</sub> hexagonal nanorings derived from Co-based metal organic frameworks. *J Mater Chem A*. 2014;2(41):17408-14.
  - Gurunathan P, Ette PM, Lakshminarasimhan N, Ramesha K. A Convenient Synthesis Route for Co<sub>3</sub>O<sub>4</sub> Hollow Microspheres and Their Application as a High Performing Anode in Li-Ion Batteries. *ACS Omega*. 2017;2(11):7647-57.
  - Yan N, Hu L, Li Y, Wang Y, Zhong H, Hu X, et al. Co<sub>3</sub>O<sub>4</sub> Nanocages for High-Performance Anode Material in Lithium-Ion Batteries. *The Journal of Physical Chemistry C*. 2012;116(12):7227-35.
  - Subalakshmi P, Sivashanmugam A. Nano Co<sub>3</sub>O<sub>4</sub> as Anode Material for Li-Ion and Na-Ion Batteries: An Insight into Surface Morphology. *ChemistrySelect*. 2018;3(18):5040-9.
  - Feng C, Zhang J, He Y, Zhong C, Hu W, Liu L, et al. Sub-3 nm Co<sub>3</sub>O<sub>4</sub> Nanofilms with Enhanced Supercapacitor Properties. *ACS Nano*. 2015;9(2):1730-9.
  - Goudarzi M, Bazarganipour M, Salavati-Niasari M. Synthesis, characterization and degradation of organic dye over Co<sub>3</sub>O<sub>4</sub> nanoparticles prepared from new binuclear complex precursors. *RSC Adv*. 2014;4(87):46517-20.
  - Teng Y, Song LX, Wang LB, Xia J. Face-Raised Octahedral Co<sub>3</sub>O<sub>4</sub> Nanocrystals and Their Catalytic Activity in the Selective Oxidation of Alcohols. *The Journal of Physical Chemistry C*. 2014;118(9):4767-73.
  - Kwak G, Hwang J, Cheon J-Y, Woo MH, Jun K-W, Lee J, et al. Preparation Method of Co<sub>3</sub>O<sub>4</sub> Nanoparticles Using Ordered Mesoporous Carbons as a Template and Their Application for Fischer-Tropsch Synthesis. *The Journal of Physical Chemistry C*. 2013;117(4):1773-9.
  - Wang Q, Xia Y, Jiang C. Mesoporous nanobelts and nano-necklaces of Co<sub>3</sub>O<sub>4</sub> converted from β-Co(OH)<sub>2</sub> nanobelts via a thermal decomposition route for the electrocatalytic oxidation of H<sub>2</sub>O<sub>2</sub>. *CrystEngComm*. 2014;16(41):9721-6.
  - Khalaji AD, Jarosova M, Machek P, Chen K, Xue D. Li-ion battery studies on nickel oxide nanoparticles prepared by facile route calcination. *Polyhedron*. 2020;179:114360.
  - Khalaji AD, Jarosova M, Machek P, Chen K, Xue D. Facile synthesis, characterization and electrochemical performance of nickel oxide nanoparticles prepared by thermal decomposition. *Scripta Materialia*. 2020;181:53-7.
  - Petríček V, Dušek M, Palatinus L. Crystallographic Computing System JANA2006: General features. *Zeitschrift für Kristallographie - Crystalline Materials*. 2014;229(5).
  - Cheary RW, Coelho AA. Axial Divergence in a Conventional X-ray Powder Diffractometer. II. Realization and Evaluation in a Fundamental-Parameter Profile Fitting Procedure. *Journal of Applied Crystallography*. 1998;31(6):862-8.
  - Zhang XX, Xie QS, Yue GH, Zhang Y, Zhang XQ, Lu AL, et al. A novel hierarchical network-like Co<sub>3</sub>O<sub>4</sub> anode material for lithium batteries. *Electrochimica Acta*. 2013;111:746-54.
  - Zhong M, He W-W, Shuang W, Liu Y-Y, Hu T-L, Bu X-H. Metal-Organic Framework Derived Core-Shell Co/Co<sub>3</sub>O<sub>4</sub>@N-C Nanocomposites as High Performance Anode Materials for Lithium Ion Batteries. *Inorganic Chemistry*. 2018;57(8):4620-8.
  - Ding H, Zhang X-K, Fan J-Q, Zhan X-q, Xie L, Shi D, et al. MOF-Templated Synthesis of Co<sub>3</sub>O<sub>4</sub>@TiO<sub>2</sub> Hollow Dodecahedrons for High-Storage-Density Lithium-Ion Batteries. *ACS Omega*. 2019;4(8):13241-9.
  - Chen K, Xue D. Crystallization of transition metal oxides within 12 seconds. *CrystEngComm*. 2017;19(8):1230-8.
  - Chen K, Xue D. Colloidal supercapattery. *SCIENTIA SINICA Technologica*. 2018;49(2):175-81.
  - Hu P, Zhao D, Liu H, Chen K, Wu X. Engineering PPy decorated MnCo<sub>2</sub>O<sub>4</sub> urchins for quasi-solid-state hybrid capacitors. *CrystEngComm*. 2019;21(10):1600-6.
  - Zhang Y-Z, Wang Y, Xie Y-L, Cheng T, Lai W-Y, Pang H, et al. Porous hollow Co<sub>3</sub>O<sub>4</sub> with rhombic dodecahedral structures for high-performance supercapacitors. *Nanoscale*. 2014;6(23):14354-9.
  - Jin L, Li X, Ming H, Wang H, Jia Z, Fu Y, et al. Hydrothermal synthesis of Co<sub>3</sub>O<sub>4</sub> with different morphologies towards efficient Li-ion storage. *RSC Advances*. 2014;4(12):6083.
  - Ren M, Yuan S, Su L, Zhou Z. Chrysanthemum-like Co<sub>3</sub>O<sub>4</sub> architectures: Hydrothermal synthesis and lithium storage performances. *Solid State Sciences*. 2012;14(4):451-5.